processes

MDPI

Article

Feasibility of Basalt Fiber Felt as Biocarrier for Rural Domestic Wastewater Treatment: Performance and Microbial Community Analysis

Qian Xu [1,2], Yuxuan Zhai [1], Jilong Gao [1], Hai Lin [1] and Yunmeng Pang [1,*]

[1] School of Energy and Environmental Engineering, University of Science and Technology Beijing, Beijing 100083, China; x1483616397@163.com (Q.X.); m202420254@xs.ustb.edu.cn (Y.Z.); m202520220@xs.ustb.edu.cn (J.G.); linhai@ces.ustb.edu.cn (H.L.)
[2] School of Ecological and Environmental Sciences, East China Normal University, Shanghai 200241, China
* Correspondence: pangym@ustb.edu.cn

Abstract

In response to the intermittent discharge and frequent flow interruptions characteristic of rural domestic wastewater, this study evaluated the treatment performance and microbial mechanisms of basalt fiber (BF) felt as a novel biofilm carrier, with comparative analyses against traditional polyurethane (PU) carrier. Under continuous-flow conditions, both carriers showed no significant difference in the removal efficiencies of COD and NH_4^+-N. However, when switching to intermittent feeding mode with flow interruption, the BF reactor maintained high removal efficiencies for pollutants (COD, NH_4^+-N and TN removals averaged 90.5%, 89.4% and 64.5%, respectively), significantly outperforming the PU reactor (COD, NH_4^+-N and TN removals averaged 82.3%, 32.7% and 20.7%, respectively). High-throughput sequencing results revealed that the BF carrier significantly enriched nitrifiers (e.g., *Nitrospira*) and aerobic denitrifiers (e.g., *Terrimonas* and *Bacillus*) during the intermittent operation phase. Functional prediction further indicated increased abundances of functional genes associated with nitrification (*amoA*, *hao*), complete denitrification (*narG*, *nosZ*), as well as glycolysis (*GAPDH*) and the TCA cycle (*IDH1*, *korA*) related to NADH generation, suggesting an enhanced coupling mechanism of carbon and nitrogen metabolism in the BF system. Conversely, a significant reduction in microbial diversity and the abundance of relevant functional genes was observed on the traditional carriers. This study confirms that BF felt, serving as a biocarrier for rural domestic wastewater treatment, exhibits superior shock load resistance and nitrogen removal performance, which provides an efficient and reliable carrier option for decentralized wastewater treatment in rural areas.

Keywords: basalt fiber carrier; intermittent flow; rural domestic wastewater; bacterial community; C and N metabolism

Check for updates

Academic Editor: Shaoan Cheng

Received: 8 December 2025
Revised: 7 January 2026
Accepted: 15 January 2026
Published: 19 January 2026

Copyright: © 2026 by the authors. Licensee MDPI, Basel, Switzerland. This article is an open access article distributed under the terms and conditions of the Creative Commons Attribution (CC BY) license.

1. Introduction

Rural domestic wastewater has emerged as a pressing environmental concern. Centralized collection is often prohibited by dispersed settlement patterns, leading to widespread direct discharge of untreated wastewater and consequent environmental contamination [1]. In contrast to municipal wastewater, rural domestic wastewater is characterized by decentralized sources and considerable fluctuations in influent quality [2]. Particularly distinctive is its intermittent discharge pattern, which peaks three times daily (morning, noon, and evening) with notably elevated volumes during holidays, while flow may cease entirely

during off-peak periods [3,4]. These unique attributes render conventional wastewater treatment systems often inadequate, underscoring the need for approaches suited to the practical conditions of rural settings.

For decentralized rural wastewater treatment, biofilm-based processes have emerged as a leading technology due to their strong resistance to shock loads and low sludge production [5]. Within these systems, the biofilm carrier is a critical determinant of performance, as its physicochemical characteristics, such as specific surface area, porosity, and surface charge, significantly influence microbial adhesion, growth, and colonization [6]. Biofilm carriers are commonly categorized into organic and inorganic types. Organic carriers are predominantly synthetic polymer-based materials, such as polyvinyl alcohol (PVA), polyvinyl chloride (PVC), polystyrene (PS), and polyurethane (PU) [7]. Inorganic carriers include zeolite, ceramic particles, activated carbon, and similar materials [8]. While effective in continuous-flow municipal systems, these conventional carriers face a key limitation in rural scenarios. Under intermittent and frequently interrupted flow conditions, attached microorganisms experience alternating feast–famine cycles, leading to inefficient pollutant removal and potential biofilm inactivation during dry periods.

Therefore, developing biofilm carriers capable of adapting to the intermittent discharge patterns of rural wastewater is crucial for mitigating the adverse impacts of flow interruptions and optimizing treatment performance. In recent years, basalt fiber (BF) has been explored as a promising alternative inorganic carrier material [9,10]. BF is an inorganic, eco-friendly material produced by melting volcanic rock and drawing it into filaments using a platinum-rhodium alloy [11]. It exhibits high porosity and specific surface area, with main chemical components including SiO_2, Al_2O_3, CaO, MgO, and TiO_2, alongside high mechanical strength and corrosion resistance [12] (Bhat et al., 2018). Owing to its high porosity, BF can create localized micro-water-retaining environments [13], which may alleviate microbial dehydration and inactivation during flow cessation, showing promising potential for application in rural wastewater biofilm systems.

Research has demonstrated the efficacy of BF as a carrier in continuous-flow bioreactors treating various wastewaters, including municipal sewage and landfill leachate, achieving high removal efficiencies for chemical oxygen demand (COD) and total nitrogen (TN) by facilitating favorable microenvironments for simultaneous nitrification and denitrification [13–15]. Ni et al. [13] constructed a biological contact oxidation reactor using BF as the carrier to treat simulated municipal sewage at a hydraulic retention time (HRT) of 24 h, achieving COD removal efficiency above 90% and TN removal ranging from 60% to 82%, indicating considerable denitrification capability. In another study, Ni et al. [14] employed a BF-based biological contact oxidation reactor to treat landfill leachate. Under HRT = 10 h, COD and TN removal efficiency reached 86.9% and 76.7%, respectively [14]. Further research demonstrated that modified BF with enhanced surface hydrophilicity promotes microbial adhesion more effectively [10].

Despite this promising potential, a significant research gap remains. Existing studies have predominantly processed BF into fibrous carriers for application in continuous-flow reactors [9,13,14]. Its specific application and performance in intermittent-flow fixed-bed biofilm reactors designed for rural domestic wastewater treatment have not been reported. Furthermore, the characteristics of microbial community succession on BF felt under alternating dry-wet conditions, as well as the underlying organic and nitrogenous pollutants removal mechanisms, remain unclear.

To address these gaps, this study aims to construct fixed-bed biofilm reactor using BF felt as the carrier material. The primary objectives are (1) to investigate and compare the pollutant removal performance of BF-based bioreactor with traditional PU-based bioreactor under intermittent flow and flow interruption conditions representative of rural settings;

and (2) to elucidate the underlying removal mechanisms by analyzing the microbial community composition via high-throughput sequencing and predicting functional gene profiles within the biofilms. The results are expected to provide scientific support for the optimization of carrier materials in biofilm-based treatment of rural domestic wastewater.

2. Materials and Methods

2.1. Materials

Basalt fiber (BF) felt (BHT Environmental Technology Co., Ltd., Beijing, China) and Polyurethane (PU) sponge (Shen Yuan Water Treatment Filler Co., Ltd., Zhengzhou, China) were used in the experiment. They were cut into 20 × 20 × 20 mm cubes to serve as biocarriers for the experiments. The porosity of both carriers was tested by mercury intrusion porosimetry (MIP). The BF carrier had a porosity of 91.2% and a total pore surface area of 0.27 m^2/g, whereas the corresponding values for the conventional PU carrier were 33.3% and 0.08 m^2/g, respectively (Table 1). The pore size distribution of BF felt was concentrated with an average pore size of 56,675 nm (Table S1). In contrast, the pore size distribution of PU was relatively broad, ranging from 553 nm to 374,905 nm, with an average pore size of 21,957 nm.

Table 1. Physical properties of the BF and PU biocarriers.

Physical Properties	BF	PU
Total pore volume (mL/g)	3.83	0.43
Total pore surface area (m^2/g)	0.27	0.08
Average pore diameter (nm)	56,675.31	21,957.85
Bulk density (g/mL)	0.24	0.77
Skeletal density (g/mL)	2.71	1.16
Porosity (%)	91.22	33.34

2.2. Biofilter Reactor Design

The biofilter reactors were constructed from plexiglass in a cylindrical shape, with an inner diameter of 8.5 cm and a height of 13 cm (Figure 1). The carrier packing height was 11 cm, resulting in an effective volume of 0.63 L. An air diffuser was installed at the bottom of each reactor. Aeration was supplied at a rate of 20 mL/min, controlled by a gas flowmeter. Simulated domestic wastewater was delivered at a constant flow rate into the two experimental columns using peristaltic pumps, with the inflow rate regulated by liquid flowmeters.

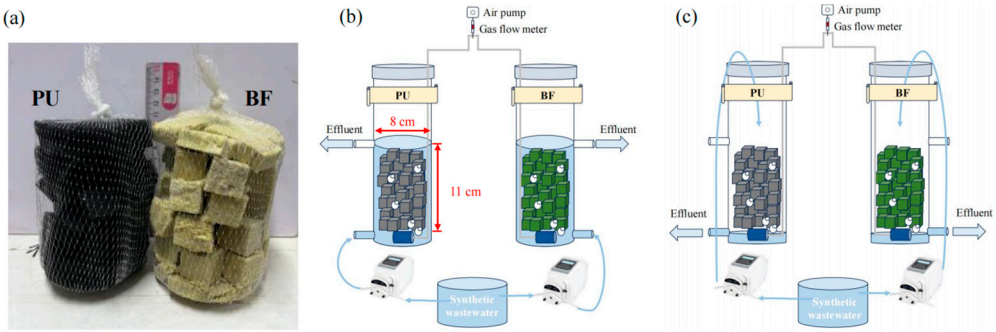


Figure 1. Macro-morphology of the biocarriers (**a**) and schematic diagrams of the biofilter under continuous-flow (**b**) and intermittent-flow (**c**) configurations.

2.3. Reactor Startup and Operation

The inoculating activated sludge during the startup phase was collected from the Gaobeidian Wastewater Treatment Plant in Beijing. After initial feeding, the reactors un-

derwent static aeration for 3 days before formal operation. Phase I of the experiment (Day 0–30) employed a continuous-flow operation mode with "downward influent and upward effluent". The HRT was progressively reduced from 12 h (Day 0–7) to 8 h (Day 8–14), 4 h (Day 15–22), and 2 h (Day 23–30). To better simulate the intermittent discharge characteristics of rural domestic wastewater, Phase II was switched to an intermittent-flow and flow-interruption mode with "upward influent and downward effluent" (Day 31–55).

The simulated rural domestic wastewater used in the experiment was consisted of $C_6H_{12}O_6$, $(NH_4)_2SO_4$, and KH_2PO_4 as the organic, nitrogen, and phosphorus pollutants, respectively. In addition, 1 ‰ (v/v) trace element solution was supplied to the influent, and the composition is detailed in the supporting information.

Under the continuous-flow operation mode (Phase I), the main pollutant concentrations were: COD = 300 mg/L, NH_4^+-N = 20 mg/L, TP = 3 mg/L. Under the intermittent-flow mode (Phase II), high-load and low-load conditions were established to better represent fluctuations in rural wastewater pollutant concentrations. The high-load condition (Day 31–42) maintained the same concentrations as Phase I, while the low-load condition (Day 43–55) was set at COD = 150 mg/L, NH_4^+-N = 15 mg/L, and TP = 1.5 mg/L.

During the intermittent-inflow phase simulating rural usage, influent was supplied only during four daily time windows (7:00–9:00, 11:00–13:00, 16:00–18:00, 20:00–22:00), with reactors otherwise held in a no-flow state.

2.4. Chemical Analyses

During reactor operation, influent and effluent samples were collected daily. After filtration through a 0.22 μm membrane filter, the water quality parameters, including COD, pH, ammonium nitrogen (NH_4^+-N), nitrite nitrogen (NO_2^--N), and nitrate nitrogen (NO_3^--N), were analyzed. Specifically, COD concentration was determined using the rapid COD analyzer (5B-3A, Lianhua Technology Co., Ltd., Beijing, China) and pH was measured with the pH meter (S220, Mettler-Toledo Inc., Zurich, Switzerland). NH_4^+-N concentration was quantified by Nessler spectrophotometry at 420 nm with the UV-Vis spectrophotometer (GENESYS 180, Thermo Fisher Scientific Inc., Waltham, MA, USA). NO_2^--N concentration was determined through N-(1-naphthyl)-ethylenediamine dihydrochloride spectrophotometry at 540 nm, and NO_3^--N concentration was analyzed by ultraviolet spectrophotometry at 220 nm with correction at 275 nm. NH_4^+-N, NO_2^--N and NO_3^--N were all determined with the UV-Vis spectrophotometer (GENESYS 180, Thermo Fisher Scientific Inc., Waltham, MA, USA).

2.5. Microbial Analyses

Biofilm samples attached to carriers from the middle section of both reactors were collected during the startup phase, continuous-flow phase (Day 14), and intermittent-flow phase (Day 55). The samples were processed by Majorbio Bio-pharm Technology Co., Ltd., Shanghai, China. for 16S rRNA high-throughput sequencing analysis. DNA was extracted from the biofilm samples using the DNA extraction kit M5635-02 (Omega Bio-Tek Inc., Norcross, GA, USA). The V3–V4 region of the bacterial 16S rRNA gene was amplified using the primer set 338F and 806R. Following PCR, the purified amplicons were sequenced on the Illumina NovaSeq 6000 platform (Illumina Inc., San Diego, CA, USA). Raw sequence data were subjected to quality filtering and denoising using the QIIME 2 platform (v2023.9, https://qiime2.org). Using UPARSE software (v7.0.1001), the remaining high-quality sequences were clustered into operational taxonomic units (OTUs) at a 97% sequence identity threshold. The α-diversity indices (Chao, ACE, Shannon, and Inv-Simpson) were calculated based on OTU richness. Principal coordinate analysis (PCoA) was performed using the Bray–Curtis distance matrix in R 3.3.1 with the vegan package. The relative

abundances of metabolic pathways and functional genes were predicted using PICRUSt2 (v2.2.0) based on the KEGG database [16].

3. Results and Discussion

3.1. Continuous-Flow Performance

3.1.1. COD Removal Performance Under Continuous-Flow Conditions

Throughout the operational period, the influent COD concentration fluctuated between 252.8 mg/L and 337.1 mg/L. During the HRT = 12 h phase, the effluent COD removal efficiencies of both carriers stabilized above 90%, indicating that under continuous-flow conditions, both carriers could achieve rapid biofilm formation within a relatively short timeframe. Subsequently, as HRT was reduced from 12 h to 8 h and then to 4 h, the COD removal rates in both reactors were largely unaffected. At HRT = 4 h, the average effluent COD concentrations for the BF and PU reactors were 25.0 mg/L and 22.4 mg/L, respectively, corresponding to average removal efficiencies of 91.6% and 92.7% (Figure 2), and average COD removal rates of 70.60 mg/L/h and 71.53 mg/L/h. During the continuous-flow phase at HRT ranging from 4 to 12 h, both carriers demonstrated effective COD removal performance.

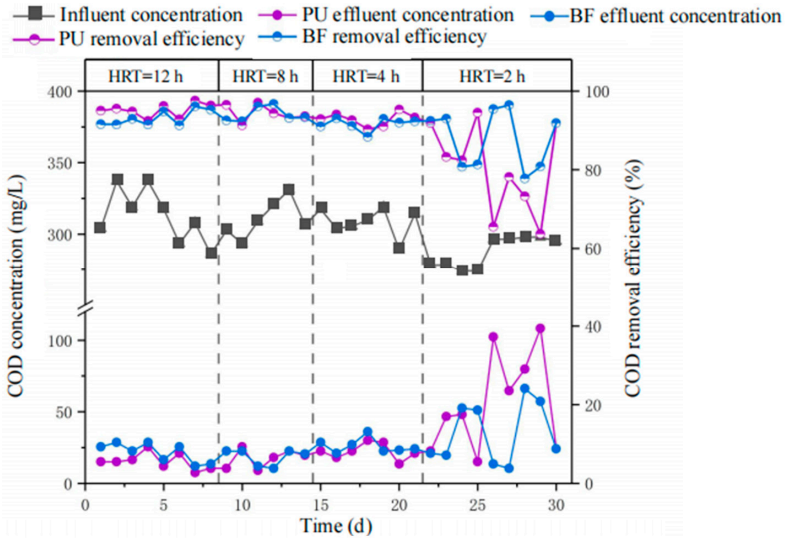


Figure 2. COD removal performance under continuous-flow condition.

When HRT was further reduced to 2 h, the COD removal efficiency of the PU reactor was significantly impacted, with the average efficiency decreasing to 78.3% and a minimum value of only 61.6%. In contrast, the BF reactor maintained an average COD removal efficiency of 87.1% under the HRT = 2 h condition. This indicates that under low HRT conditions, BF as a carrier exhibits superior performance compared to PU.

The COD removal rate of the BF reactor in this study compares favorably with reported systems treating similar synthetic rural wastewater. While Xu et al. [5] achieved a COD removal rate of 15.8 mg/(L·h) at 24 h HRT in a moving bed biofilm reactor (MBBR), and Cheng et al. [17] reported 47.7 mg/(L·h) at 2 h HRT in a waterwheel-driven rotating biological contactor (WRBC), the BF reactor attained a higher rate of 130 mg/(L·h) at 2 h HRT. This suggests that the present system may offer an efficiency advantage under substantially shortened retention times.

3.1.2. Nitrogen Removal Performance Under Continuous-Flow Conditions

Both the BF and PU reactors achieved their optimal nitrogen removal performance at an HRT of 4 h. During this phase, with a stable influent NH_4^+-N concentration around

20 mg/L, the average NH_4^+-N removal efficiencies for the BF and PU reactors were both higher than 90% (Figure 3). In the effluents of both the BF and PU reactors, slight accumulations of NO_2^--N and NO_3^--N nitrogen were observed. This indicates that after NH_4^+-N was oxidized to NO_2^--N, complete denitrification for NO_3^--N removal was not achieved.

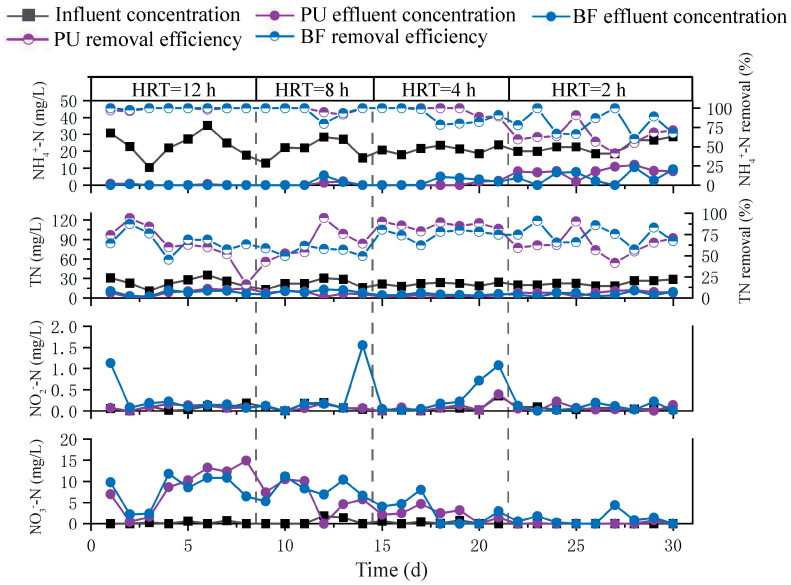


Figure 3. NH_4^+-N and TN removal performance under continuous-flow condition.

However, when the HRT was reduced to 2 h, the average removal rates of NH_4^+-N and TN in the PU reactor decreased significantly to 63.2% and 63.1%, respectively. In contrast, the average removal rates in the BF reactor only declined slightly to 79.4% and 75.9%. Concurrently, the accumulation of NO_2^--N and NO_3^--N markedly decreased. Consistent with the COD removal results, the BF carrier demonstrated superior performance compared to the PU carrier under low HRT conditions.

Compared with previous studies, the BF reactor also demonstrates comparable nitrogen removal performance. In the MBBR reactor studied by Xu et al. [5], the average removal efficiencies for NH_4^+-N and TN were 85.6% and 81.7%, respectively, at an HRT of 24 h. In contrast, this study achieved a similar removal level at a significantly shorter HRT of only 4 h. The effluent quality from the BF reactor in this study met the discharge standards (Grade I) for rural wastewater in some provinces in China, which stipulate COD $\leq$ 50 mg/L, NH_4^+-N $\leq$ 5 mg/L, and TN $\leq$ 15 mg/L.

3.2. Intermittent-Flow Performance

3.2.1. COD Removal Performance Under Intermittent-Flow Conditions

Under the intermittent-flow mode, the reactors operated in a trickling filter configuration. Except during the four daily influent periods (each lasting 2 h), the reactors remained in a flow-interruption state. Consequently, during the initial phase following the operational change, the COD removal performance of both reactors was adversely affected.

When the influent COD was 300 mg/L (Day 31–42), the COD removal rates of the BF and PU reactors fluctuated between 71.4–94.5% and 76.4–92.5%, respectively (Figure 4). After the influent COD concentration in the intermittent operation was reduced to 150 mg/L (Day 43–55), the COD removal efficiency of the BF reactor (averaging 90.5%) was significantly superior to that of the PU reactor (averaging 82.3%).

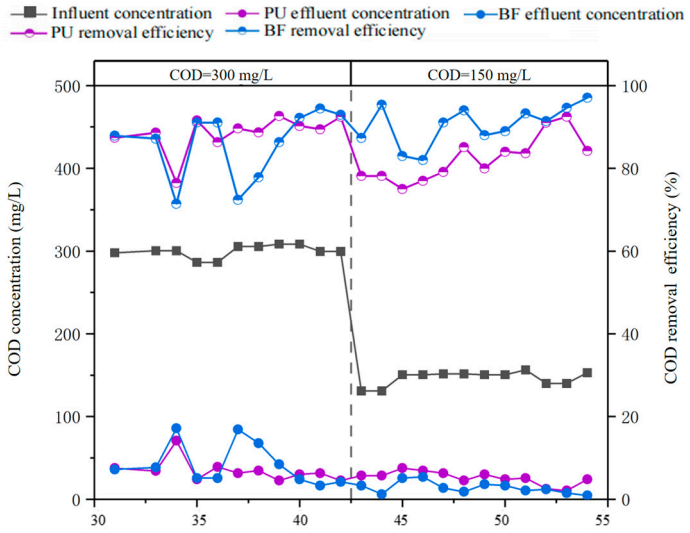


Figure 4. COD removal performance under intermittent-flow condition.

In the intermittent-flow with flow-interruption mode, the BF reactor demonstrated better COD removal performance compared to the PU reactor. This is primarily attributed to the fact that the intermittent-flow and interruption left the carriers exposed to air for most of the time, further shortening the contact duration between the wastewater and the microorganisms. The extremely high porosity and microscale pore size of the BF carrier might enable the formation of localized micro-water-retaining niches. This allowed it to remain moist even during non-feeding periods, providing a more favorable habitat for the microorganisms.

3.2.2. Nitrogen Removal Performance Under Intermittent-Flow Conditions

Compared to COD removal, the intermittent-flow with flow-interruption mode had a more pronounced impact on nitrogen removal performance. The PU reactor exhibited poor NH_4^+-N removal, with efficiency consistently below 50%. In contrast, after a 7-day adaptation period, the BF reactor showed a significant improvement in NH_4^+-N removal, achieving a maximum efficiency of 99.6% and an average of 89.4% (Figure 5).

During the first stage of intermittent-flow operation (Day 31–42), the effluent NO_3^--N concentration from both reactors remained relatively low. However, a gradual increase in effluent NO_3^--N concentration was observed after 42 days. This increase may be attributed to two factors: the gradual adaptation and enhanced activity of nitrifying bacteria in the reactors, leading to greater NO_3^--N production; concurrently, the influent C/N ratio decreased from approximately 15 in the first stage to about 10 in the second stage (Day 43–55). A lower C/N ratio is less favorable for denitrifying bacteria [18]. Therefore, the rise in effluent NO_3^--N concentration during the second stage likely resulted from weakened denitrification.

Regarding NO_2^--N, after 12 days of intermittent-flow operation, significant NO_2^--N accumulation was observed in the PU reactor, with a maximum effluent concentration reaching 2.1 mg/L. In contrast, the effluent NO_2^--N concentration from the BF reactor remained consistently lower than 0.44 mg/L.

At a C/N ratio of approximately 15, the average TN removal rate of the BF reactor was 68.2%, representing only a 7.7% decrease compared to the continuous-flow mode. For the PU reactor, however, the average TN removal rate was merely 37.5%. When the C/N ratio decreased to about 10, the average TN removal rate of the BF reactor was 60.7%, whereas that of the PU reactor further declined to 3.9%. In the PU reactor, almost all NH_4^+-N was converted to NO_2^--N or NO_3^--N without subsequent denitrification,

indicating that the intermittent-flow with flow-interruption mode is unfavorable for the proliferation of denitrifying bacteria. When using conventional PU as the biofilm carrier under intermittent-flow conditions, the carrier is exposed to air for most of the time, making it difficult to form anoxic zones within the carrier to support the growth and activity of denitrifying bacteria [19], thereby resulting in weak denitrification. In contrast, the BF felt carrier, due to its unique pore structure, may facilitate the formation of multi-layered aerobic–anoxic biofilm structures within its interior [13], promoting processes such as simultaneous nitrification and denitrification and partial nitrification–denitrification.

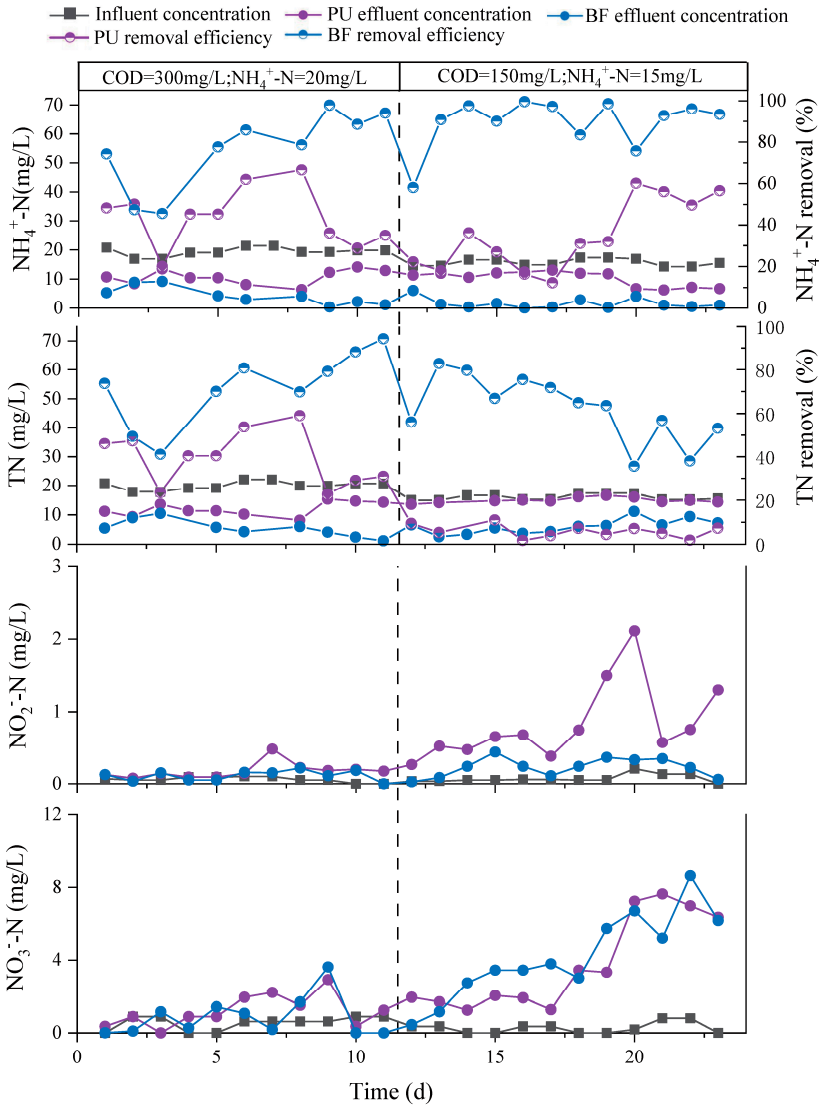


Figure 5. NH_4^+-N and TN removal performance under intermittent flow.

Compared to conventional biocarriers (e.g., PU, PE, PP, ceramic particles, zeolite), the BF carrier demonstrates superior pollutant removal under intermittent-flow and comparable operational conditions (Table S3), which closely represent rural wastewater discharge patterns. In addition, BF offers favorable material characteristics, including high mechanical strength, corrosion resistance, and low density. Environmentally, it is a non-toxic inorganic material with minimal leaching risk. Economically, BF is cost-effective and exhibits long-term stability due to its inorganic nature. In summary, BF felt represents a promising and compatible biofilm carrier for intermittent-flow rural wastewater treatment.

3.3. Microbial Community Succession

Biofilm samples collected from the BF and PU reactors during the startup phase, continuous-flow phase and intermittent-flow phase were labeled as BF1, BF2, BF3 and PU1, PU2, PU3, respectively. High-throughput sequencing of the six samples yielded a total of 41,308 valid sequences. The numbers of operational taxonomic units (OTUs) obtained for these samples were 1335, 1548, 1497, 1370, 1281 and 828, respectively.

3.3.1. Microbial Community Diversity

Alpha diversity analysis (Figure 6) indicated a significant decrease in the Shannon, Inv-Simpson, Chao, and ACE indices for PU3 compared to PU2. In contrast, no significant differences were observed between BF3 and BF2. These results demonstrate that the diversity and richness of the microbial community on the PU carrier markedly declined during the intermittent-flow phase, whereas the microbial community on the BF carrier remained relatively stable.

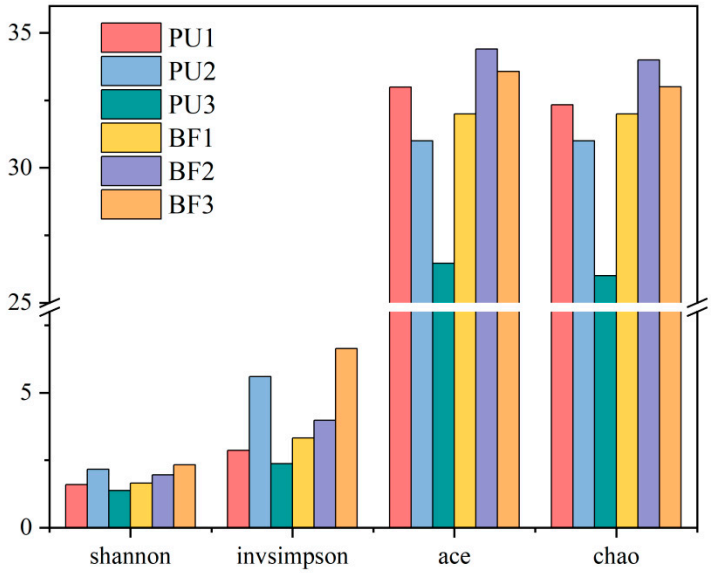


Figure 6. Alpha diversity index of biofilms on different biocarriers. BF1, BF2, BF3, PU1, PU2, and PU3 represent the biofilm samples collected from the BF and PU reactors during the startup phase, continuous-flow phase, and intermittent-flow phase, respectively.

The observed decrease in microbial diversity within the PU reactor under intermittent-flow conditions suggests that flow interruption adversely affected the growth of a portion of the microbial population established during the continuous-flow operation. Microbial community diversity is strongly associated with the functional stability and resilience of a wastewater treatment system [20]. Typically, biofilm systems with higher diversity and richness exhibit greater operational stability [21]. Therefore, the maintained high diversity in the BF reactor implies that the BF carrier provided a more favorable micro-environment for microbial attachment and growth under intermittent-flow with interruption conditions compared to the traditional carrier. This finding aligns with the superior COD and TN removal performance of the BF reactor observed under the same operational mode.

3.3.2. Microbial Community Composition

Principal Coordinates Analysis (PCoA) revealed that the microbial community structures on the two carriers were similar during the startup phase (Figure 7a). However, as operational conditions changed, the composition of the biofilm microbial community on

the PU carrier exhibited considerable variation, whereas that on the BF carrier showed relatively minor shifts.

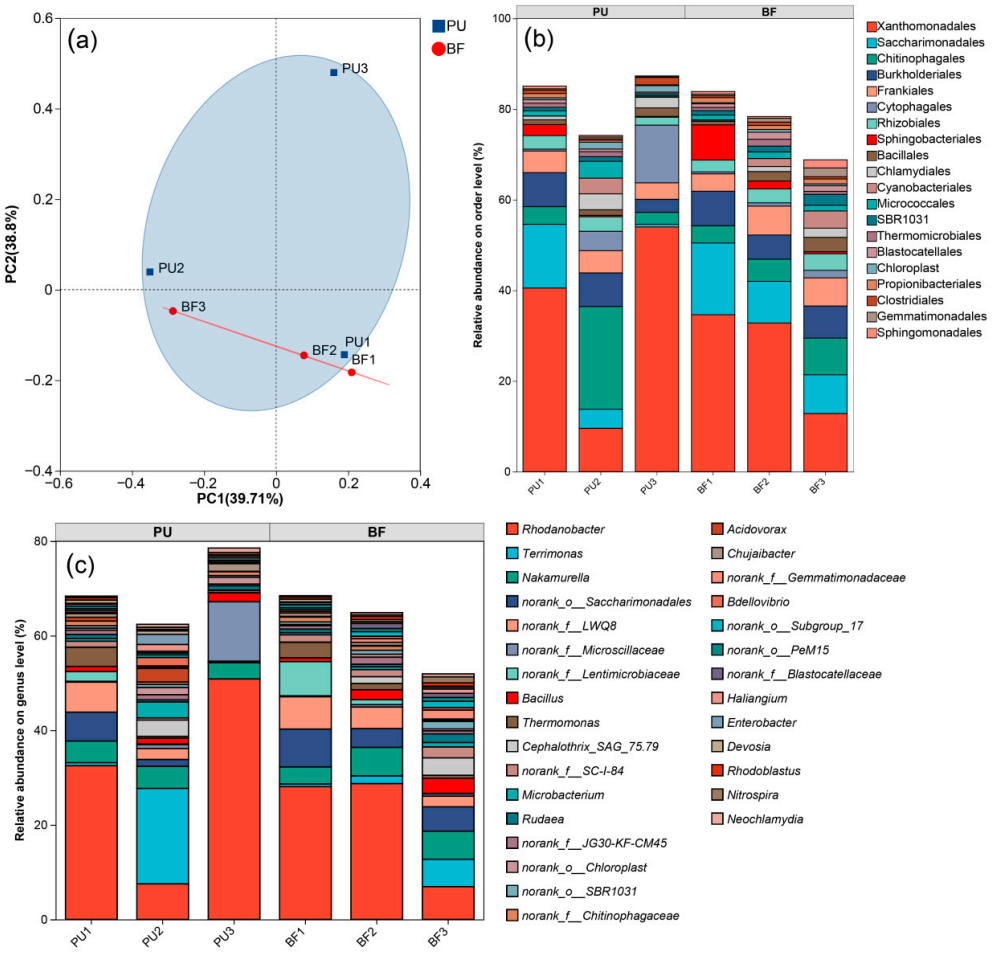


Figure 7. (**a**) PCoA analysis (based on OTUs) of the bacteria community in different biofilm samples. Relative abundances at order (**b**) and genus (**c**) level.

At the phylum level, Proteobacteria was the most abundant phylum across all samples, followed by Bacteroidota and Actinobacteriota. This distribution is consistent with the typical community structure of biofilm systems treating domestic wastewater, where Proteobacteria are widely recognized for their metabolic versatility, particularly in aerobic organic carbon oxidation and key nitrogen transformations such as nitrification and denitrification [22].

At the order level, Xanthomonadales, Saccharimonadales, Chitinophagales, Burkholderiales, and Frankiales were identified as the dominant orders, with their relative abundances varying considerably among different samples. When the operational mode shifted from continuous-flow to intermittent-flow, the relative abundance of Xanthomonadales on the PU carrier increased from 9.6% to 54.0%, while it decreased from 32.8% to 12.8% on the BF carrier (Figure 7b). Bacteria within the order Xanthomonadales are predominantly aerobic heterotrophs known for their capacity to degrade complex organic compounds and reduce COD [23]. In contrast, the relative abundance of Saccharimonadales on the PU carrier declined from 4.2% to 0.6%, whereas it remained relatively stable on the BF carrier. Furthermore, the relative abundance of Burkholderiales decreased on the PU carrier but increased on the BF carrier. Bacteria belonging to the orders Saccharimonadales and Burkholderiales are primarily facultative anaerobes, many of which possess denitrification capabilities [24,25].

These results indicate that after switching from continuous-flow to intermittent-flow mode, aerobic bacteria were substantially enriched on the PU carrier, while the abundances of some facultative anaerobic bacteria with denitrification potential were significantly reduced. Conversely, both aerobic and anaerobic bacteria remained dominant in the BF carrier. This discrepancy was probably attributed to the high porosity of the BF felt, which might promote the formation of localized micro-water-retention environments during flow interruption periods, thereby supporting the concurrent growth of both aerobic and anaerobic microorganisms.

At genus level, certain denitrifying bacteria such as *Terrimonas* and *Bacillus* were significantly enriched on the BF carrier under intermittent-flow conditions. Their relative abundances increased by 3.6-fold and 1.5-fold, respectively, which were substantially higher than those observed on the PU carrier (Figure 7c). Notably, some species within the genus *Bacillus* possess heterotrophic nitrification and aerobic denitrification capabilities [26]. Furthermore, the relative abundance of the nitrifying bacterium *Nitrospira* on the BF carrier increased from 0.3% under continuous-flow conditions to 1.3% under intermittent-flow conditions, whereas its abundance on the PU carrier remained at only 0.4%. *Nitrospira* is an autotrophic bacterium with a relatively long generation time [27]. Its enrichment on the BF carrier even under intermittent-flow conditions further demonstrates the superiority of the BF carrier.

In summary, the microbial community structure analysis indicates that the community on the BF carrier was more stable compared to that on the PU carrier and exhibited a stronger ability to enrich both nitrifying and denitrifying bacteria under intermittent-flow conditions.

3.4. Functional Gene Abundance

The predicted abundances of genes involved in nitrogen (N) and carbon (C) metabolism are shown in Figure 8.

3.4.1. N Cycling Functional Genes

Regarding N metabolism, genes associated with nitrification (*amoA*, *hao*), denitrification (*napA*, *narG*, *nirS*, *nirK*, *norB*, *nosZ*), dissimilatory nitrate reduction to ammonium (DNRA; *nrfA*, *nirB/D*), and nitrate assimilation (*nasA*, *nirA*) were detected in all samples from both BF and PU carriers.

Specifically, the relative abundances of the genes *amoA* and *hao*, which are responsible for ammonia oxidation to nitrite [28], progressively increased on the BF carrier. During the intermittent-flow phase, their abundances on the BF carrier were 203% and 92% higher, respectively, than during the continuous-flow phase, and 316% and 251% higher than those on the PU carrier (Figure 7b). For denitrification, genes driving the reduction of NO_3^- to NO_2^- (*narG*), NO to N_2O (*norB*), and N_2O to N_2 (*nosZ*) were also significantly enriched on the BF carrier, showing increases of 41%, 23%, and 51%, respectively, compared to the continuous-flow phase. In addition to nitrification and denitrification genes, DNRA and nitrate assimilation genes (*nirB/D* and *nasA*) were substantially enriched on the BF carrier during the intermittent-flow phase. In contrast, the relative abundances of these N cycling functional genes on the PU carrier under intermittent-flow conditions were markedly lower than those under continuous-flow conditions. This was particularly evident for nitrification genes (*amoA*, *hao*), denitrification genes (*narG*, *napA*, *nirS*, *norB*, *nosZ*), and the nitrate assimilation gene (*nasA*).

These results indicate that the intermittent-flow with interruption mode had negligible adverse effects on the nitrogen transformation functional potential of the microbial community on the BF carrier. Instead, the N transformation capacity was enhanced over

time. However, for the conventional PU carrier, flow interruption significantly inhibited the growth and functional activity of N cycling microorganisms. These provide a robust explanation for the superior NH_4^+-N and TN removal performance observed in the BF reactor compared to the PU reactor under intermittent-flow condition.

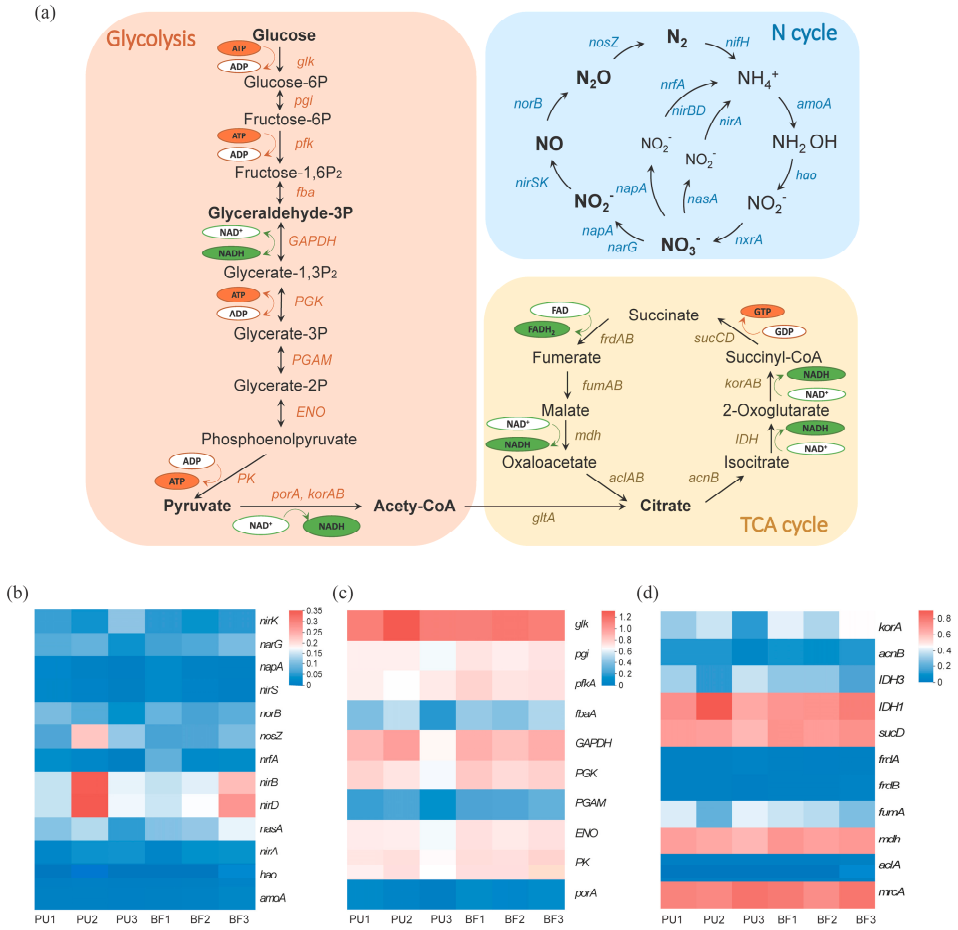


Figure 8. (**a**) An overview of genes involved in N cycle, glycolysis and TCA cycle. Relative abundance (‰) of genes for N cycle (**b**), glycolysis (**c**) and TCA cycle (**d**) in different biofilm samples.

3.4.2. C Cycling Functional Genes

Glycolysis and the TCA cycle are key pathways for energy generation in C metabolism [22]. Glucose is degraded to pyruvate via glycolysis, then converted to acetyl-CoA, which subsequently enters the TCA cycle and is ultimately oxidized to CO_2 through respiration. The electron donors required for denitrification are derived from NADH generated during glycolysis and the TCA cycle [22]. Consequently, the functional genes involved in C metabolism are closely linked with those involved in N metabolism.

Regarding the glycolysis process, most gene abundances showed no significant differences between the BF and PU carriers. However, the relative abundance of the *GAPDH* gene on the BF carrier increased from 0.84‰ during continuous-flow to 0.91‰ under intermittent-flow, while on the PU carrier it decreased from 0.96‰ to 0.67‰ (Figure 7c). *GAPDH* is a key gene catalyzing the conversion of glyceraldehyde-3-phosphate to 1,3-bisphosphoglycerate, a step that also generates the electron carrier NADH [29]. Furthermore, the relative abundance of the *porA* gene, which drives the conversion of pyruvate to acetyl-CoA [30], increased on the BF carrier from 0.068‰ during continuous flow to 0.098‰ under intermittent flow, whereas on the PU carrier it decreased from 0.050‰ to 0.015‰.

For the TCA cycle, the relative abundances of the genes *IDH1* (catalyzing the conversion of isocitrate to 2-oxoglutarate) and *korA* (catalyzing the conversion of 2-oxoglutarate to succinyl-CoA) on the BF carrier under intermittent flow increased by 3.9% and 29%, respectively. In contrast, these abundances on the PU carrier decreased by 13.5% and 62.0% (Figure 8d). Both of these steps are also key processes for NADH generation [31]. Furthermore, the relative abundance of the *acnB* gene, responsible for isocitrate synthesis, increased by 35.6% on the BF carrier but decreased by 54.4% on the PU carrier.

In summary, these results indicate that intermittent-flow with interruption suppressed the electron carrier (NADH) generation function associated with microbial C metabolism on the conventional PU carrier, while its impact on the BF carrier was minimal. The microbial community on the BF carrier thus maintained a guaranteed supply of NADH, which provided sufficient electrons to support microbial denitrification. Consequently, in the BF reactor, NH_4^+-N oxidized to NO_3^--N via nitrification could be efficiently reduced to gaseous N through denitrification, thereby sustaining a high TN removal rate.

4. Conclusions

This study demonstrates the significant advantages of basalt fiber (BF) felt as a biocarrier for rural domestic wastewater treatment. Under conditions simulating the intermittent inflow and flow interruption characteristic of rural wastewater, the BF carrier exhibited remarkable resistance to shock loads, achieving average removal efficiencies of 90.5% for COD, 89.4% for NH_4^+-N, and 64.5% for TN, significantly outperforming the conventional polyurethane (PU) carrier. Mechanistic investigations revealed that the BF carrier effectively enriched nitrifying bacteria and aerobic denitrifiers, while maintaining higher microbial diversity. Furthermore, the abundance of key functional genes associated with nitrification, denitrification, and carbon metabolism was significantly enhanced in the BF system, reinforcing the coupling of carbon and nitrogen metabolic pathways. The insights gained into the microbial community structure and metabolic functions offer a mechanistic understanding that paves the way for its future engineering implementation.

Supplementary Materials: The following supporting information can be downloaded at: https://www.mdpi.com/article/10.3390/pr14020349/s1, Figure S1: Pore size distribution curve of the BF (a) and PU (b) carrier; Table S1: Trace element solution composition; Table S2: Methods for water quality parameter determination; Table S3: Comparison of different biocarriers, refs. [8,32].

Author Contributions: Conceptualization, Q.X. and Y.P.; methodology, Q.X. and Y.P.; validation, Q.X. and Y.P.; formal analysis, Y.Z. and J.G.; investigation, Q.X.; resources, H.L.; data curation, Y.Z. and J.G.; writing—original draft preparation, Q.X.; writing—review and editing, Y.P. and H.L.; visualization, Y.Z. and J.G.; supervision, Y.P.; project administration, H.L.; funding acquisition, Y.P. All authors have read and agreed to the published version of the manuscript.

Funding: This research was funded by the National Natural Science Foundation of China (42007215).

Data Availability Statement: The original contributions presented in this study are included in the article or Supplementary Material. Further inquiries can be directed to the corresponding author.

Conflicts of Interest: The authors declare no conflicts of interest.

References

1. Liu, J.G.; Zhou, Z.Y.; Li, P.Y.; Wang, Z.X.; Yan, Y.; Yu, X.Z.; Li, W.K.; Zheng, T.L.; Cao, Y.N.; Wu, W.J.; et al. Characteristics of rural domestic sewage discharge and their driving mechanisms: Evidence from the Northern Region, China. *Front. Environ. Sci. Eng.* **2024**, *18*, 83. [CrossRef]
2. Wang, C.; Feng, B.B.; Wang, P.F.; Guo, W.Z.; Li, X.J.; Gao, H.; Zhang, B.; Chen, J. Revealing factors influencing spatial variation in the quantity and quality of rural domestic sewage discharge across China. *Process Saf. Environ. Prot.* **2022**, *162*, 200–210. [CrossRef]

3. Li, X.Y.; Zhang, X.; Zhao, M.; Zheng, X.Y.; Wang, Z.Q.; Fan, C.Z. Application of Decentralized Wastewater Treatment Technology in Rural Domestic Wastewater Treatment. *Sustainability* **2024**, *16*, 8635. [CrossRef]
4. Xie, Y.D.; Zhang, Q.H.; Wu, Q.; Zhang, J.Y.; Dzakpasu, M.; Wang, X.C. Novel adaptive activated sludge process leverages flow fluctuations for simultaneous nitrification and denitrification in rural sewage treatment. *Water Res.* **2024**, *255*, 121535. [CrossRef]
5. Xu, B.; Wang, H.; Zhang, H.; Pu, M.; Zhao, M.; Tadayuki, F.; Zheng, X. Optimization of MBBR performance for rural domestic wastewater: Effects of carrier type, operating conditions, and zooplankton regulation. *Process Saf. Environ. Prot.* **2025**, *202*, 107847. [CrossRef]
6. Zhao, Y.X.; Liu, D.; Huang, W.L.; Yang, Y.; Ji, M.; Nghiem, L.D.; Trinh, Q.T.; Tran, N.H. Insights into biofilm carriers for biological wastewater treatment processes: Current state-of-the-art, challenges, and opportunities. *Bioresour. Technol.* **2019**, *288*, 121619. [CrossRef] [PubMed]
7. Morgan-Sagastume, F. Biofilm development, activity and the modification of carrier material surface properties in moving-bed biofilm reactors (MBBRs) for wastewater treatment. *Crit. Rev. Environ. Sci. Technol.* **2018**, *48*, 439–470. [CrossRef]
8. Lago, A.; Rocha, V.; Barros, O.; Silva, B.; Tavares, T. Bacterial biofilm attachment to sustainable carriers as a clean-up strategy for wastewater treatment: A review. *J. Water Process Eng.* **2024**, *63*, 105368. [CrossRef]
9. Zhang, X.Y.; Zhou, X.T.; Xie, Y.J.; Rong, X.S.; Liu, Z.G.; Xiao, X.; Liang, Z.S.; Jiang, S.Y.; Wei, J.; Wu, Z.R. A sustainable bio-carrier medium for wastewater treatment: Modified basalt fiber. *J. Clean. Prod.* **2019**, *225*, 472–480. [CrossRef]
10. Zhou, Y.; Wang, X.C.; Arslan, M.; Zhou, X.T.; Wu, Z.R.; Liu, J.X.; Li, X.Y.; Din, M.G. Impact of truncated modified basalt fibers on aerobic granular sludge stability and pollutant removal in piggery wastewater treatment. *Chem. Eng. J.* **2024**, *495*, 153475. [CrossRef]
11. Ni, H.C.; Wang, C.C.; Arslan, M.; Qian, J.C.; Liang, Z.S.; Luo, Z.J.; Cai, R.Q.; El-Din, M.G.; Wu, Z.R. Enhanced wastewater treatment by modified basalt fiber bio-carriers: Effect of etching and surface functionalization. *J. Clean. Prod.* **2022**, *343*, 130927. [CrossRef]
12. Bhat, T.; Fortomaris, D.; Kandare, E.; Mouritz, A.P. Properties of thermally recycled basalt fibres and basalt fibre composites. *J. Mater. Sci.* **2018**, *53*, 1933–1944. [CrossRef]
13. Ni, H.C.; Zhou, X.T.; Zhang, X.Y.; Xiao, X.; Liu, J.F.; Huan, H.; Luo, Z.J.; Wu, Z.R. Feasibility of using basalt fiber as biofilm Carrier to construct bio-nest for wastewater treatment. *Chemosphere* **2018**, *212*, 768–776. [CrossRef]
14. Ni, H.C.; Arslan, M.; Qian, J.; Wang, Y.; Liu, Z.; Luo, Z.; Cai, R.; EI-Din, M.G.; Wu, Z. Application of basalt fibers in a biological contact oxidation reactor for the treatment of landfill leachate. *J. Clean. Prod.* **2021**, *297*, 126648. [CrossRef]
15. Zhou, X.T.; Arslan, M.; Liu, Z.G.; Li, D.; Xi, H.P.; Feng, Y.J.; Li, S.W.; Wei, J.; Rong, X.S.; Liang, Z.S.; et al. Low carbon-to-nitrogen ratio digestate from high-rate anaerobic baffled reactor facilitates heterotrophic/autotrophic nitrifiers involved in nitrogen removal. *Bioresour. Technol.* **2022**, *359*, 127346. [CrossRef] [PubMed]
16. Douglas, G.M.; Maffei, V.J.; Zaneveld, J.R.; Yurgel, S.N.; Brown, J.R.; Taylor, C.M.; Huttenhower, C.; Langille, M.G.I. PICRUSt2 for prediction of metagenome functions. *Nat. Biotechnol.* **2020**, *38*, 685–688. [CrossRef] [PubMed]
17. Cheng, H.; Li, W.; Gong, Z.; Wen, C.; Zhang, C.; Lu, X. Treatment Performance and Characteristics of Biofilm Carriers in an Aerobic Waterwheel-Driven Rotating Biological Contactor. *Water* **2025**, *17*, 356. [CrossRef]
18. Pang, Y.; Wang, J. Various electron donors for biological nitrate removal: A review. *Sci. Total Environ.* **2021**, *794*, 148699. [CrossRef]
19. Loupasaki, E.; Diamadopoulos, E. Attached growth systems for wastewater treatment in small and rural communities: A review. *J. Chem. Technol. Biotechnol.* **2013**, *88*, 190–204. [CrossRef]
20. Pang, Y.M.; Zhai, Y.X.; Fu, Y.X.; Lin, H.; Wang, J.L. A review of antibiotic effects on wastewater denitrification: From process inhibition to microbial resistance mechanism. *Process Saf. Environ. Prot.* **2025**, *201*, 107590. [CrossRef]
21. Allison, S.D.; Martiny, J.B.H. Resistance, resilience, and redundancy in microbial communities. *Proc. Natl. Acad. Sci. USA* **2008**, *105*, 11512–11519. [CrossRef] [PubMed]
22. Yang, Z.; Zhou, Q.; Sun, H.; Jia, L.; Zhao, L.; Wu, W. Metagenomic analyses of microbial structure and metabolic pathway in solid-phase denitrification systems for advanced nitrogen removal of wastewater treatment plant effluent: A pilot-scale study. *Water Res.* **2021**, *196*, 117067. [CrossRef] [PubMed]
23. Brunings, A.M.; Gabriel, D.W. Xanthomonas citri: Breaking the surface. *Mol. Plant Pathol.* **2003**, *4*, 141–157. [CrossRef]
24. Pang, Y.M.; Xia, L.; Li, S.J.; Wang, J.L.; Lin, H. Metagenomic insights into a solid phase heterotrophic-autotrophic denitrification reactor driven by biodegradable polymers and pyrite. *J. Clean. Prod.* **2025**, *523*, 146411. [CrossRef]
25. Tan, H.; Wang, L.; Chen, Y.W.; Li, X.; Zhou, H.Z.; Tan, Z.L. Revealing the differences in metabolisms and nitrogen removal mechanisms of the full and shortcut nitrification-denitrification processes for the treatment of livestock wastewater. *J. Environ. Chem. Eng.* **2024**, *12*, 112381. [CrossRef]
26. Kim, J.K.; Park, K.J.; Cho, K.S.; Nam, S.W.; Park, T.J.; Bajpai, R. Aerobic nitrification-denitrification by heterotrophic Bacillus strains. *Bioresour. Technol.* **2005**, *96*, 1897–1906. [CrossRef]
27. Young, B.; Delatolla, R.; Abujamel, T.; Kennedy, K.; Laflamme, E.; Stintzi, A. Rapid start-up of nitrifying MBBRs at low temperatures: Nitrification, biofilm response and microbiome analysis. *Bioprocess Biosyst. Eng.* **2017**, *40*, 731–739. [CrossRef]
28. Zhao, Y.; Li, W.G.; Chen, L.; Zhou, Y.J. Characterization of heterotrophic nitrification by a thermotolerant *Brevibacillus Agri* N_2 isolated from sewage sludge composting. *Environ. Res.* **2022**, *214*, 113903. [CrossRef]

29. Pang, Y.; Wang, J. Effect of ferric iron (Fe(III)) on heterotrophic solid-phase denitrification: Denitrification performance and metabolic pathway. *Bioresour. Technol.* **2023**, *369*, 128401. [CrossRef]
30. Ivanov, V.; Stabnikov, V.; Zhuang, W.Q.; Tay, J.H.; Tay, S.T.L. Phosphate removal from the returned liquor of municipal wastewater treatment plant using iron-reducing bacteria. *J. Appl. Microbiol.* **2005**, *98*, 1152–1161. [CrossRef] [PubMed]
31. Qian, Y.F.; Xu, M.Y.; Deng, T.C.; Hu, W.Z.; He, Z.L.; Yang, X.A.; Wang, B.; Song, D.; Chen, L.T.; Huang, Y.D.; et al. Synergistic interactions of Desulfovibrio and Petrimonas for sulfate-reduction coupling polycyclic aromatic hydrocarbon degradation. *J. Hazard. Mater.* **2021**, *407*, 124385. [CrossRef] [PubMed]
32. Al-Amshawee, S.; Yunus, M.Y.B.M.; Vo, D.V.N.; Tran, N.H. Biocarriers for biofilm immobilization in wastewater treatments: A review. *Environ. Chem. Lett.* **2020**, *18*, 1925–1945. [CrossRef]

Disclaimer/Publisher's Note: The statements, opinions and data contained in all publications are solely those of the individual author(s) and contributor(s) and not of MDPI and/or the editor(s). MDPI and/or the editor(s) disclaim responsibility for any injury to people or property resulting from any ideas, methods, instructions or products referred to in the content.